European Journal of Medicinal Chemistry 143 (2018) 503–514

Contents lists available at ScienceDirect

European Journal of Medicinal Chemistry

journal homepage: http://www.elsevier.com/locate/ejmech

Research paper

Novel ruthenium methylcyclopentadienyl complex bearing a bipyridine perfluorinated ligand shows strong activity towards colorectal cancer cells

Ricardo G. Teixeira [a], Ana Rita Brás [a, b], Leonor Côrte-Real [a], Rajendhraprasad Tatikonda [c], Anabela Sanches [a], M. Paula Robalo [d, e], Fernando Avecilla [f], Tiago Moreira [a, b], M. Helena Garcia [a], Matti Haukka [c], Ana Preto [b], Andreia Valente [a, *]

[a] Centro de Química Estrutural, Faculdade de Ciências da Universidade de Lisboa, Campo Grande, 1749-016 Lisboa, Portugal
[b] Centre of Molecular and Environmental Biology (CBMA), Department of Biology, University of Minho, Portugal, Campus de Gualtar, Braga 4710-057, Portugal
[c] Department of Chemistry, Nanoscience Center, University of Jyväskylä, P. O. Box 35, FI-40014 Jyväskylä, Finland
[d] Área Departamental de Engenharia Química, ISEL-Instituto Superior de Engenharia de Lisboa, Instituto Politécnico de Lisboa, Rua Conselheiro Emídio Navarro, 1, 1959-007 Lisboa, Portugal
[e] Centro de Química Estrutural, Complexo I, Instituto Superior Técnico, Universidade de Lisboa, Av. Rovisco Pais, 1049-001 Lisboa, Portugal
[f] Grupo Xenomar, Centro de Investigacións Científicas Avanzadas (CICA), Departamento de Química, Facultade de Ciencias, Universidade da Coruña, Campus de A Coruña, 15071 A Coruña, Spain

ARTICLE INFO

Article history:
Received 25 September 2017
Received in revised form
6 November 2017
Accepted 21 November 2017

Keywords:
Ruthenium methylcyclopentadienyl
Colorectal cancer
Apoptosis
Selectivity

ABSTRACT

Three new compounds have been synthesized and completely characterized by analytical and spectroscopic techniques. The new bipyridine-perfluorinated ligand **L1** and the new organometallic complex [Ru(η^5-MeCp)(PPh_3)$_2$Cl] (**Ru1**) crystalize in the centrosymmetric triclinic space group P$\bar{1}$. Analysis of the phenotypic effects induced by both organometallic complexes **Ru1** and [Ru(η^5-MeCp)(PPh_3)(**L1**)][CF_3SO_3] (**Ru2**), on human colorectal cancer cells (SW480 and RKO) survival, showed that **Ru2** has a potent anti-proliferative activity, 4–6 times higher than cisplatin, and induce apoptosis in these cells. Data obtained in a noncancerous cell line derived from normal colon epithelial cells (NCM460) revealed an intrinsic selectivity of **Ru2** for malignant cells at low concentrations, showing the high potential of this compound as a selective anticancer agent.

1. Introduction

Ruthenium arene complexes have emerged in the last years as promising alternatives to the traditional platinum-based drugs in the frame of chemotherapy [1–4]. In general, ruthenium complexes seem to induce less side effects than platinum drugs, having different modes of action and being many times also active against metastases [1–4]. Two main families of these organometallic compounds bearing {Ru(η^6-arene)} [2,5] and {Ru(η^5-cyclopentadienyl)} [6] scaffolds have been identified. All these organometallic compounds have a piano-stool structure, where three of the coordination sites are occupied by the (η^6-arene) or the (η^5-cyclopentadienyl) ligands, which serve to stabilize the Ru(II) centre. The three remaining coordination sites are occupied by several *co*-ligands that are able to modulate the cytotoxicity and stability of the compounds. The first family comprises the ruthenium(II)-arene RAPTA-type, [Ru(η^6-arene)(PTA)X_2] (PTA = 1,3,5-triaza-7-phosphaadamantane) and the RAED-type compounds, [Ru(η^6-arene)(en)Cl]$^+$ (en = ethylenediamine) [5]. Several RAPTA compounds have revealed *in vitro* and *in vivo* anticancer activity and some of them show antimetastatic potential as well [5,7]. The RAED compounds have shown important cytotoxicity against a wide panel of human cancer cell lines [8] and [Ru(η^6-biphenyl)(en)Cl]$^+$ showed *in vivo* reduction of the MCa mammary primary carcinoma and also on the development and growth of lung metastases [9].

Relatively to the {Ru(η^5-cyclopentadienyl)} family of compounds, some have been distinguished as protein kinase inhibitors [10–12], namely for the GSK3, Pim1 and PAK1 with IC_{50} values of

* Corresponding author.
E-mail address: amvalente@fc.ul.pt (A. Valente).

https://doi.org/10.1016/j.ejmech.2017.11.059
0223-5234/

~1 μM. The need of more water soluble {Ru(η^5-cyclopentadienyl)} agents led to the synthesis of compounds incorporating water soluble phosphane ligands [13–19] in their structure. These compounds have shown moderate [18] to good [13,17–19] cytotoxicity against several cancer cell lines. The RuCp family of complexes bearing heteroaromatic ligands is the most extensive one [6,20–29]. In this frame, we have selected the $[RuCp(N,X)PPh_3]^+$ general structure (where N,X is a bidentate ligand coordinated by two nitrogen or a nitrogen and an oxygen atom) as the most promising scaffold in terms of cytotoxic properties and stability [6]. These compounds have showed excellent IC_{50} values in several human cancer cell lines with different degrees of aggressiveness and also resistant to cisplatin (*eg.*: PC3, MCF7, MDAMB231, A2780, A2780CisR, HeLa, between others) [6]. Preliminary *in vivo* studies for a compound of this family, $[RuCp(N,O)PPh_3]^+$ (N,O = 2-benzoylpyridine) [21], on nude mice bearing orthotopic triple negative breast cancer MDAMB231, proved the potential of these complexes by suppressing tumour growth comparatively to the controls and by inhibiting the formation of metastases [30]. These results undoubtedly show that further studies regarding these compounds should be undertaken.

It is known that the incorporation of fluorine in bioactive molecules improve their pharmacological properties through the enhancement of metabolic stability, changes in their physicochemical properties or increasing binding affinities, resulting in an enhancement of their therapeutic efficacy [31,32]. In the frame of cancer, 5-Fluoruacil (5-FU) has recognized tumour-inhibiting activity [33]. One of the best properties introduced by fluorine relies on the increased lipid solubility, which improves the rates of absorption and transport of drugs *in vivo*. Recently, compounds bearing perfluorinated chains coupled to ruthenium-*p*-cymene [34,35] and RAPTA derivatives such as [Ru(η^6-arene)(pta)(PR_3)Cl] BF_4 (arene = *p*-cymene or 4-phenyl-2-butanol; PR_3 = perfluorinated phosphanes) [36] showed considerable antiproliferative activity and some of them were found to be thermoresponsive towards cancer cells. [(η^6-$C_{10}H_{14}$)RuCl(MFPdpm or PFPdpm)] and [(η^6-$C_{12}H_{18}$)Ru-Cl (MFPdpm or PFPdpm)] (MFPdpm = 5-(4-fluoro)phenyldipyrromethene; PFPdpm = 5-(penta-fluoro)phenyldipyrromethene) compounds also exhibited good cytotoxicity towards human lung cancer cell line (A549) [37]. Taking these results into consideration we report here for the first time the synthesis of a bipyridine bearing two perfluorinated chains and the synthesis of the corresponding ruthenium-(η^5-MeCp) complex. As far as we know these compounds are unexplored in the frame of anticancer agents.

2. Experimental section

2.1. General procedures

All reactions and manipulations were performed under nitrogen atmosphere using *Schlenk* techniques. All solvents used were dried and freshly distilled under nitrogen prior to use, using standard methods [38]. ^{1}H, ^{13}C, ^{19}F and ^{31}P NMR spectra were recorded on a Bruker Avance 400 spectrometer at probe temperature using commercially available deuterated solvents. ^{1}H and ^{13}C chemical shifts (s = singlet; d = duplet; t = triplet; m = multiplet; comp = complex) are reported in parts per million (ppm) downfield from internal standard Me_4Si. ^{19}F and ^{31}P NMR spectra are reported in ppm downfield from external standard $CFCl_3$ and 85% H_3PO_4, respectively. Coupling constants are reported in Hz. All assignments were attributed using DEPT-135, COSY, HMBC and HMQCNMR techniques. Infrared spectra were recorded on KBr pellets using a Mattson Satellite FT-IR spectrophotometer. Only considered relevant bands were cited in the text. Electronic spectra were obtained at room temperature on a Jasco V-560 spectrometer from solutions of 10^{-4}-10^{-6} M in quartz cuvettes (1 cm optical path). Elemental analyses were performed at *Laboratório de Análises, at Instituto Superior Técnico*, using a Fisons Instruments EA1 108 system. Data acquisition, integration and handling were performed using a PC with the software package EAGER-200 (Carlo Erba Instruments).

2.2. Synthesis

2.2.1. perFluor-bpy ***(L1)***

The ligand synthesis was carried out by following the literature procedure [39] with slight modifications using 4,4′-dihydroxy-2,2′-bipyridine as starting material instead of 4′-hydroxy-2,2′:6′,2″-terpyridine. A mixture of 4,4′-dihydroxy-2,2′-bipyridine (95 mg, 0.5 mmol), K_2CO_3 (207 mg, 1.5 mmol), a catalytic amount of 18-crown-6 in 30 mL of acetone was stirred at room temperature for 1 h. After that, ^{1}H,^{1}H,^{2}H,^{2}H,^{3}H,^{3}H-Perfluoroundecyl iodide (589 mg, 1 mmol) dissolved in 5 mL of acetone was added dropwise to the reaction mixture at room temperature. The reaction mixture was refluxed for 2 days. After the reaction time, the reaction mixture was cooled to room temperature and white crystalline product was filtered and washed with an excess amount of water and acetone and dried under vacuum.

Yield: 67%. White flaky product. Mp: 150.5–153.2 °C. ^{1}H NMR ($CDCl_3$, Me_4Si, δ/ppm): 8.38 (d, 2H, J_{HH} = 5.6, H_5), 7.84 (d, 2H, J_{HH} = 2.5, H_8), 6.88 (dd, 2H, J = 5.6, 2.5, H_6), 4.36 (t, 4H, J_{HH} = 5.9, H_{10}), 2.51 (m, 4H, H_{12}), 2.35 (m, 4H, H_{11}). ^{1}H NMR ($CDCl_3$ + 2 drops of HFIP, Me_4Si, δ/ppm): 8.39 (d, 2H, J_{HH} = 5.9, H_5), 7.62 (d, 2H, J_{HH} = 2.4, H_8), 6.95 (dd, 2H, J = 5.9, 2.5, H_6), 4.22 (t, 4H, J_{HH} = 5.9, H_{10}), 2.39–2.25 (m, 4H, H_{12}), 2.21–2.15 (m, 4H, H_{11}). ^{1}H NMR ($(CD_3)_2CO$, Me_4Si, δ/ppm): 8.50 (d, 2H, J_{HH} = 5.1, H_5), 8.08 (s, 2H, H_8), 7.03–7.00 (m, 2H, H_6), 4.40–4.04 (m, 4H, H_{10}), 2.56 (m, 4H, H_{12}). ^{13}C NMR [$CDCl_3$ + 2 drops of HFIP, δ/ppm]: 166.61, 157.11, 150.00, 125.97, 123.16, 120.33, 117.52, 111.64, 109.12, 67.03, 29.87, 27.87, 20.44. ^{19}F NMR [$CDCl_3$ + 2 drops of HFIP, δ/ppm]: −58.83, −92.31, −99.71, −99.92, −100.12, −101.42, −104.11. FTIR [KBr, cm^{-1}]: 3080–2889 ($\upsilon_{C\text{-}H}$ aromatic), 1458 ($\upsilon_{C\text{-}C}$ aromatic), 1334 (υ_{CF} stretch). ESI-TOF Mass: Calcd. for $C_{32}H_{19}F_{34}N_2O_2$ $[M+H]^+$ = 1109.0898, found = 1109.0870. Elemental analysis (%) calc. for $C_{32}H_{18}F_{34}N_2O_2$ (1108.44): C, 34.7; H, 1.6, N, 2.5. Found: C, 34.4; H, 2.0; N, 2.3.

2.2.2. [Ru(η^5-MeCp)(PPh_3)$_2$Cl] ***(Ru1)***

The synthesis of **Ru1** was adapted from Ref. [40]. To a stirred and degassed solution of hydrated ruthenium trichloride (0.5 g, 2.4 mmol) in ethanol (50 mL) was added triphenylphosphane (2.89 g, 11 mmol) and freshly distilled methylcyclopentadiene (5–6 mL). The dark brown mixture obtained was refluxed with vigorously stirring for 8 h until no more precipitation of the orange complex is observed. After refluxing, the mixture was cooled to room temperature overnight. The precipitate was filtered, washed with water (2 × 20 mL), cold ethanol (2 × 20 mL) and a mixture of ethanol and light petroleum ether (50:50 (%v/v), 2 × 20 mL). The orange powder obtained was dried under vacuum originating **Ru1** in moderate yield. Single crystals were isolated by recrystallization from dichloromethane/*n*-hexane.

Yield: 48%; orange powder, recrystallized from dichloromethane/*n*-hexane. Mp: *ca.* 145 °C decomposition. ^{1}H NMR [$CDCl_3$, Me_4Si, δ/ppm]: 7.37 (t, 12H, J_{HH} = 8.2, H_{meta},PPh_3), 7.21 (t, 6H, J_{HH} = 7.2, H_{para},PPh_3), 7.11 (t, 12H, J_{HH} = 7.4, H_{ortho},PPh_3), 3.96 (s, 2H, H_3), 3.26 (s, 2H, H_4), 1.92 (s, 3H, H_1). ^{13}C NMR [$CDCl_3$, δ/ppm]: 138.73 (Cq, PPh_3), 133.94 (CH, PPh_3), 128.68 (CH, PPh_3), 127.50 (CH, PPh_3), 104.93 (C_2), 80.95 (C_3), 76.69 (C_4), 12.03 (C_1). ^{31}P NMR [$CDCl_3$, δ/ppm]: 40.11 [s, PPh_3]. FTIR [KBr, cm^{-1}]: 2920-2852 cm^{-1} ($\upsilon_{C\text{-}H}$

aromatic). UV–vis [DMSO, λ_{max}/nm (ε/$M^{-1}cm^{-1}$)]: 289 (*Sh*), 336 (*Sh*), 386 (*Sh*), 448 (*Sh*). UV–vis [CH_2Cl_2, λ_{max}/nm (ε/$M^{-1}cm^{-1}$)]: 289 (*Sh*), 361 (2394), 450 (*Sh*). Elemental analysis (%) calc. for $C_{42}H_{37}ClP_2Ru$ (740.21): C, 68.1; H, 5.0. Found: C, 67.8; H, 5.0.

2.2.3. [Ru(η^5-MeCp)(**L1**)(PPh_3)][CF_3SO_3] (**Ru2**)

L1 (0.300 g, 0.3 mmol) and $AgCF_3SO_3$ (0.094 g, 0,4 mmol) were added to a stirred solution of Ru(η^5-MeCp)(PPh_3)$_2$Cl] (0.262 g, 0,4 mmol) in dichloromethane (40 mL). After refluxing for 4 h the solution turned from orange to brown. AgCl and PPh_3 precipitate were eliminated from the solution by cannula filtration and the solvent removed by vacuum. Forced precipitations from dichloromethane/*n*-hexane mixture allowed the isolation of the pure complex **(Ru2)**.

Yield: 31%; brown powder, precipitated from dichloromethane/*n*-hexane. Mp: *ca.* 90.4 °C decomposition. ^{1}H NMR [$(CD_3)_2CO$, Me_4Si, δ/ppm]: 9.16 (d, 2H, J_{HH} = 8, H_5), 7.82 (d, 2H, J_{HH} = 2.4, H_8), 7.41 (t, 3H, J_{HH} = 8, H_{para},PPh_3), 7.33 (t, 6H, J_{HH} = 8, H_{orto},PPh_3), 7.14 (t, 6H, J_{HH} = 8 H_{meta},PPh_3), 7.02 (dd, 2H, J_{HH} = 6.5, 2.6, H_6), 4.63 (s, 2H, H_4), 4.51 (m, 2H, H_3), 4.39 (m, 4H, H_{10}), 2.47 (m, 4H, H_{12}), 2.15 (m, 4H, H_{11}) 1.66 (s, 3H, H_1). ^{13}C NMR [$(CD_3)_2CO$, δ/ppm]: 166.25 (C_7), 158.07 (C_9), 157.22 (C_5), 133.90 and 129.29 (d, J_{CP} = 11.2; d, J_{CP} = 9.5, CH-PPh_3), 133.36 (d, $^1J_{CP}$ = 40.4, Cq- PPh_3), 130.69 (d, $^4J_{CP}$ = 1.8, CH-PPh_3), 114.26 (C_6), 110.23 (C_8), 102.53 (C_2), 76.00 (C_4), 75.80 (C_3), 68.63 (C_{10}), 28.03 (C_{12}), 20.85 (C_{11}), 11.83 (C_1), 133.56 + 133.16+123.91 + 120.71 (C_{13}-C_{20}). ^{31}P NMR [$(CD_3)_2CO$, δ/ppm]: 51.50 [s, PPh_3]. ^{19}F NMR [$(CD_3)_2CO$, δ/ppm]: −78.83, −81.65, −114.77, −122.24/-122,44, −123.27, −123.93, −126.73. FTIR [KBr, cm^{-1}]: 3078–2893 (υ_{C-H} aromatic), 1250 (υCF_3SO_3 counter ion), 1342 (υ_{CF} stretch). UV–vis [DMSO, λ_{max}/nm (ε/$M^{-1}cm^{-1}$)]: 274 (27136), 293 (*Sh*), 345 (*Sh*), 420 (4628), 475 (*Sh*). UV–vis [CH_2Cl_2, λ_{max}/nm (ε/$M^{-1}cm^{-1}$)]: 271 (23211), 292 (*Sh*), 342 (*Sh*), 419 (4100), 473 (*Sh*). Elemental anal. (%) Calc. for $C_{57}H_{40}F_{37}N_2O_5PRuS\cdot\frac{1}{2}C_6H_{14}$: C, 41.3; H, 2.7; N, 1.6; S, 1.8. Found: C, 41.3; H, 2.5; N, 1.2; S, 2.0.

2.3. X-ray crystal structure determination

The crystal of **L1** was immersed in cryo-oil, mounted in a MiTeGen loop, and measured at 123 K on a Rigaku Oxford Diffraction Supernova using Cu Kα (λ = 1.54184 Å) radiation. The *CrysAlisPro* [41] program package was used for cell refinement and data reduction. A Gaussian absorption correction (*CrysAlisPro* [41]) was applied to the intensities before structure solution. The structure was solved by charge flipping method using the *SUPERFLIP* [42] software. Structural refinement was carried out using *SHELXL-2015* [43]. All H-atoms were positioned geometrically and constrained to ride on their parent atoms, with C-H = 0.93–0.97 Å and U_{iso} = 1.2•U_{eq} (parent atom).

Three-dimensional X-ray data for [RuCl(MeCp)(PPh_3)$_2$]·CH_2Cl_2 (**Ru1**) were collected on a Bruker SMART Apex CCD diffractometer at 100(2) K, using a graphite monochromator and Mo-K_α radiation (λ = 0.71073 Å) by the ϕ-ω scan method. Reflections were measured from a hemisphere of data collected of frames each covering 0.3° in ω. A total of 76661 reflections were measured, all of which were corrected for Lorentz and polarization effects and for absorption by semi-empirical methods based on symmetry-equivalent and repeated reflections. Of the total, 6873 independent reflections exceeded the significance level $|F|/\sigma(|F|) > 4.0$. After data collection, in each case a multi-scan absorption correction (SADABS) [44] was applied, and the structure was solved by direct methods and refined by full matrix least-squares on F^2 data using SHELX suite of programs [45]. The structure was solved by direct methods and refined by full-matrix least-squares methods on F^2. The non-hydrogen atoms were refined with anisotropic thermal parameters in all cases. Hydrogen atoms were included in calculation positions and refined in the riding mode. A final difference Fourier map showed a residual density outside next to the chlorine atom of solvent molecule, which was not refined: 1.406 and −0.710 e.Å^{-3}. A weighting scheme w = 1/[$\sigma^2(F_o^2)$ + (0.047100 P)^2 + 1.180300 P] for **Ru1,** where P = ($|F_o|^2 + 2|F_c|^2$)/3, was used in the latter stages of refinement. CCDC No. 1535674 and 1493775 contain the supplementary crystallographic data for **Ru1** and **L1**, respectively. These data can be obtained free of charge via http://www.ccdc.cam.ac.uk/conts/retrieving.html, or from the Cambridge Crystallographic Data Centre, 12 Union Road, Cambridge CB2 1EZ, UK; fax: (+44) 1223-336-033; or e-mail: deposit@ccdc.cam.ac.uk. Crystal data and details of the data collection and refinement for the new compounds were collected in Table 1.

2.4. Electrochemical experiments

The cyclic voltammograms were obtained at room temperature using a EG&G Princeton Applied Research Potentiostat/Galvanostat Model 273A equipped with Electrochemical PowerSuite v2.51 software for electrochemical analysis, in anhydrous acetonitrile or dichloromethane with tetrabutylammonium hexafluorophosphate (0.1 and 0.2 M) as supporting electrolyte. The electrochemical cell was a homemade three electrode configuration cell with a platinum-disc working electrode (1.0 mm) probed by a Luggin capillary connected to a silver-wire pseudo-reference electrode and a platinum wire auxiliary electrode. All the potentials reported were measured against the ferrocene/ferrocenium redox couple as internal standard and normally quoted relative to SCE (using the ferrocenium/ferrocene redox couple $E_{1/2}$ = 0.46 or 0.40 V versus SCE for dichloromethane or acetonitrile, respectively). All the experiments were performed in nitrogen atmosphere. Both the sample and the electrolyte (Fluka) were dried under vacuum for several hours prior to the experiment. Reagent grade solvents were dried, purified by standard procedures and distilled under nitrogen atmosphere before use.

2.5. Stability studies in DMSO and DMSO/DMEM

For the stability studies, all the complexes were dissolved in DMSO or 2% DMSO/98% DMEM at *ca.* 1 × 10^{-4} M for **Ru1** and 8 × 10^{-5} M for **Ru2** and their electronic spectra were recorded in the range allowed by the solvents at set time intervals.

2.6. Partition coefficient determination

The lipophilicity of **Ru1** and **Ru2** was measured by the shake-flask method [46]. The *n*-octanol and the aqueous phases were mutually saturated before the experiments, using analytical grade octanol and double distilled water. The samples were dissolved in octanol (stock solution: 1.15 × 10^{-4} M for **Ru1** and 1.03 × 10^{-4} M for **Ru2**) and aliquots of the stock solution were equilibrated with water for 4 h in a mechanical shaker. The phase ratio was 2 mL/2 mL (*n*-octanol/water). After separation of the equilibrated phases (by centrifugation at 5000 rpm for 10 min) the concentration decrease of the solute was determined in the *n*-octanol phase by UV–Vis spectrophotometry at the λ_{max} of each compound (355 nm for **Ru1** and 419 nm for **Ru2**). Triplicate experiments have been performed for each complex. The concentration for each sample was determined using the calibration curve. The partition coefficients of **Ru1** and **Ru2** were calculated using the equation:

$$log\ _{o}{}_{w} = log\left(\frac{[complex]_o}{[complex]_w}\right)$$

Table 1
Crystal data and structure refinement for **L1** and [Ru(MeCp)(PPh_3)$_2$Cl]·CH_2Cl_2 (**Ru1**).

	Ru1	L1
CCDC No.	1535674	1493775
Formula	$C_{43}H_{39}Cl_3P_2Ru$	$C_{32}H_{18}F_{34}N_2O_2$
Formula weight	825.10	1108.48
T, *K*	100(2)	123(1)
Wavelength, Å	0.71073	1.54184
Crystal system	Triclinic	Triclinic
Space group	$P\bar{1}$	$P\bar{1}$
a/Å	9.7702(4)	5.3931(5)
b/Å	14.1031(5)	7.6334(8)
c/Å	14.9277(5)	24.663(3)
$\alpha/^o$	73.247(2)	92.674(9)
$\beta/^o$	72.323(2)	94.043(8)
$\gamma/^o$	78.853(2)	110.404(9)
V/Å^3	1863.93(12)	946.50(17)
Z	2	1
F_{000}	844	546
D_{calc}/g cm^{-3}	1.470	1.945
μ/mm^{-1}	0.752	2.195
$\theta/(^o)$	1.48 to 26.42	6.604–64.495
R_{int}	0.0535	0.0768
Crystal size/mm^3	0.30 × 0.21 × 0.18	0.14 × 0.06 × 0.04
Goodness-of-fit on F^2	1.124	1.030
R_1[a]	0.0301	0.0860
wR_2 (all data)[b]	0.0896	0.2229
Largest differences peak and hole (eÅ^{-3})	1.406 and −0.710	0.503 and −0.543

[a] $R_1 = \Sigma||F_o| - |F_c||/\Sigma|F_o|$.
[b] $wR_2 = \{\Sigma[w(|F_o|^2 - |F_c|^2|)^2]|/\Sigma[w(F_o^2)^2]\}^{1/2}$.

2.7. Cell lines and culture conditions

The noncancerous NCM460 cell line derived from normal colon epithelial mucosa, was obtained from INCELL's [47], and the two colorectal cancer (CRC) derived cell lines, SW480 and RKO, were obtained from American Type Culture Collection (ATCC). All cell lines were maintained at 37 °C under a humidified atmosphere containing 5% CO_2. NCM460 and SW480 cells were grown in RPMI medium and RKO cells in DMEM, both supplemented with 10% FBS and 1% penicillin/streptomycin. Cells were subcultured once a week when 80% of confluence was reached and then seeded in sterile test plates for the assays.

2.8. Compounds dilution and storage

The **Ru1** and **Ru2** compounds were dissolved in DMSO. Aliquots were prepared and stored at −20 °C, protected from light, and discharged after one month, by which time new samples were prepared.

2.9. Sulphorhodamine B (SRB) assay

RKO, SW480 and NMC460 cells were seeded at a concentration of 4 × 10^4 cells/ml, 1 × 10^5 cells/ml and 3 × 10^5 cells/ml respectively, in 24-well test plates. After 24 h of seeding, cells were incubated with different concentrations of the **Ru1** and **Ru2** compounds during 48 h. For each cell line and compound, we performed two negative controls, a control (1) in which cells were incubated only with growth medium and another DMSO control (2) in which the cells were exposed to the concentration of DMSO in which the highest concentration of the compound was dissolved (maximum of 0.1% of DMSO per well (v/v)), to discard any influence of the DMSO in the results. After 48 h of treatment, cells were fixed in ice-cold methanol containing 1% acetic acid for at least 90 min at −20 °C. Fixing solution was then removed and the plate was left air-dry at room temperature, then the fixed cells were incubated with 0.5% (w/v) SRB dissolved in 1% acetic acid for 90 min at 37 °C protected from light. After washing with 1% acetic acid and air-drying at room temperature, SRB was solubilized with 10 mM Tris pH10. Absorbance was read at 540 nm in a microplate reader (SpectraMax 340PC Molecular Devices). Results were expressed relatively to the negative control 1, which was considered as 100% of cell growth. The results were obtained from at least three independent experiments, each experiment was done in triplicate. The statistical analysis performed using one-way ANOVA test and the IC_{50} were estimated using GraphPad Prism 6 software.

2.10. Colony formation assay

SW480 and RKO cell lines were seeded, at a concentration of 500 cells/ml and 300 cells/ml, respectively, in 6-well plates. After 24 h of seeding, cells were treated with ¼ IC_{50} and IC_{50} values of **Ru2** and incubated for 48 h, when cells were washed with PBS and the medium was replaced with fresh medium. The negative control cells were treated with DMSO 0.1%. 5 days later, cells were washed with PBS and fixated with glutaraldehyde 6% (v/v) and crystal violet 0.5% (w/v) for three hours. Then, cells were washed with fresh water and the plate was left air dry. Colonies were counted using ImageJ 1.50i software. The results represent mean ± S.D. of at least three independent experiments. Statistical analysis was performed by one-way ANOVA with Turkey's multiple comparisons test. $^*P \leq 0.05$; $^{**}P \leq 0.01$; $^{***}P \leq 0.001$ compared with negative control.

2.11. TUNEL assay

The cell lines SW480 and RKO were seeded, in 6-well plates, at a concentration of 2 × 10^5 cells/ml and 8 × 10^4 cells/ml, respectively. 24 h after seeding, cells were exposed to the IC_{50} and 2 × IC_{50} values of **Ru2**. The negative control cells were treated with DMSO 0.1%. After 48 h, both floating and attached cells were collected and washed with PBS. To the resuspended pellet was added paraformaldehyde 4%, for 15 min at room temperature (RT), to fix the cells, which were then washed with PBS. Cytospins were performed using Cytospin 4 Cytocentrifuge (Thermo Fisher Scientific). Cells were then washed in PBS and permeabilized with ice-cold 0.1% Triton X-100 in 0.1% sodium citrate. TUNEL was performed using *In Situ* Cell Death Detection Kit, Fluorescein (Roche, Mannheim, Germany). Slides were mounted on Vectashield Mounting Medium with DAPI and maintained at −20 °C until visualization in a fluorescence microscope (Leica DM 5000B, Leica Microsystems, Wetzlar, Germany). Values represent mean ± S.D. of at least three independent experiments. Statistical analysis was performed by one-way ANOVA with Turkey's multiple comparisons test. $^*P \leq 0.05$; $^{**}P \leq 0.01$; $^{***}P \leq 0.001$; $^{****}P \leq 0.0001$ compared with negative control.

2.12. Cell cycle analysis

RKO and SW480 cell lines were seeded at a concentration of 8 × 10^4 cells/ml and 2 × 10^5 cells/ml, respectively, in 6-well plates. After 24 h, cells were treated with the IC_{50} and 2 × IC_{50} values of **Ru2**. The negative control cells were treated with DMSO 0.1%. 48 h later, both dead and live cells were collected, washed with PBS and fixed and permeabilized with 70% cold ethanol for 15 min. Then the cells were washed with PBS and incubated with RNase A (200 mg/mL) for 15 min at 37 °C and with propidium iodide (0.5 mg/mL) for 30 min, protected from the light, at RT before analysis on a flow cytometer. To analyze the data and quantify the amount of cells in each cell-cycle phase was used FlowJo 7.6 software. Values represent mean ± S.D. of at least three independent experiments. Statistical analysis was performed by multiple *t*-tests. . $^*P \leq 0.05$

compared with negative control.

3. Results and discussion

3.1. Synthesis

Two new ruthenium(II) organometallic compounds have been synthesized. The new [Ru(η^5-MeCp)(PPh_3)$_2$Cl] (**Ru1**) precursor was synthesized by addition of freshly distilled methylcyclopentadiene and triphenylphosphane to a stirred ethanolic solution of ruthenium trichloride, following a modified literature procedure [40] giving dark orange crystals in 48% yield. As for the new cationic complex [Ru(η^5-MeCp)(PPh_3)(**L1**)]$^+$ **Ru2**, the synthesis was performed in reflux in dichloromethane for 4 h, by σ coordination of bidentate *N*,*N per*-fluorinated chelating ligand **L1** to **Ru1**, in the presence of silver triflate (Scheme 1). Isolation of **Ru2** as a brown powder was achieved in 31% yield. The perfluorinated bipyridyl ligand **L1** was obtained by following a modified literature procedure [39] reacting 4,4′-dihydroxy-2,2′-bipyridine with C_8F_{17}-C_3H_6I perfluorinated alkyl iodide in acetone in the presence of potassium carbonate (K_2CO_3).

The formulation and purity of all the new compounds (**L1**, **Ru1** and **Ru2**) is supported by analytical data, FT-IR spectroscopy, ^{1}H, ^{13}C, ^{31}P and ^{19}F NMR spectroscopic data and elemental analyses. In the case of **L1** and **Ru1**, X-ray diffraction of single crystals was also possible (see below).

The solid state FT-IR spectra (KBr pellets) of the complexes **Ru1** and **Ru2** present the characteristic band for the methylcyclopentadienyl ring along with the phenyl aromatic rings of the bipyridine (3100-2850 cm^{-1}; also present in **L1**). Additional bands attributed to the carbon-carbon and carbon-fluorine vibrations were also found in the range of 1220–1250 cm^{-1}, for compounds **L1** and **Ru2**. The presence of the counter-ion $CF_3SO_3^-$ (~1250 cm^{-1}) in the solid state IR spectra confirms the proposed cationic nature of complex **Ru2**.

The ^{1}H NMR spectrum (in $CDCl_3$) of **L1** shows three signals at the aromatic region (δ = 8.38, 7.84 and 6.88 ppm) which arises from the three chemically non-equivalent aromatic protons of the bipyridine moiety. The CH_2 hydrogens of perfluorinated alkyl chain which is directly attached to the oxygen atom are observed as a triplet at 4.36 ppm and other two consecutive CH_2 hydrogens appeared as multiplets at 2.51 and 2.35 ppm, respectively. The ^{13}C NMR of ligand was also obtained in $CDCl_3$ by adding 2–3 drops of hexafluoro isopropanol (HFIP) to increase the solubility of the ligand and spectral data are presented in experimental section.

The ^{1}H NMR spectra of **Ru1** shows the expected signals of (η^5-MeCp) moiety at 3.96 and 3.26 ppm, corresponding to the non-equivalent protons on the Cp ring. These signals are more shielded than in the related [RuCp(PPh_3)$_2$Cl] compound (δ = 4.12 ppm in $CDCl_3$), showing the presence of the donating methyl group on the Cp ring. Evidence of the coordination of **L1** to the ruthenium centre in **Ru2** can be observed by the deshielding on the H_5 protons, adjacent to the nitrogen of the bipyridine ring, and a shielding on the H_8 protons ligand (Table 2). This effect has been already observed for related compounds, where the bipyridine is substituted at the *para*-position (relatively to the nitrogen) [26]. The displacement of the η^5-coordinated MeCp ring signals (δ = 4.63, 4.51 ppm) also confirms that the synthesis was successful and coherent with a cationic compound. The ^{13}C NMR spectra shows the same general effect observed for the protons in both complexes. A unique sharp singlet resonance corresponding to the coordinated triphenilphosphane *co*-ligand was found in the ^{31}P NMR (δ 40.1 **Ru1,** δ 50.5 **Ru2**).

3.2. UV–visible (UV–Vis) studies

3.2.1. Compounds characterization

The electronic absorption spectra of all compounds was performed in 1 × 10^{-4} to 1 × 10^{-6} M solutions of dichloromethane and/or dimethylsulfoxide. Spectra of compounds **Ru1** and **Ru2** present an intense absorption band at *ca.* 260 nm that can be attributed to the organometallic fragment {Ru(η^5-MeCp)(PPh_3)}$^+$.

Table 2
Selected ^{1}H NMR data in $CDCl_3$ or $(CD_3)_2CO$ for compounds **L1**, **Ru1** and **Ru2**.

Compound	MeCp (ppm)			Bipyridine (ppm)					
	H_1	H_3	H_4	H_5	H_6	H_8	H_{10}	H_{11}	H_{12}
Ru1[a]	1.92	3.96	3.26	_	_	_	_	_	_
L1[a]	_	_	_	8.38	6.88	7.84	4.36	2.35	2.51
L1[b]				8.50	7.03–7.00	8.08	4.40–4.04	*	2.56
Ru2[b]	1.66	4.51	4.63	9.16	7.03	7.82	4.39	2.15	2.47

*under the solvent signal.
[a] In $CDCl_3$.
[b] In $(CD_3)_2CO$.

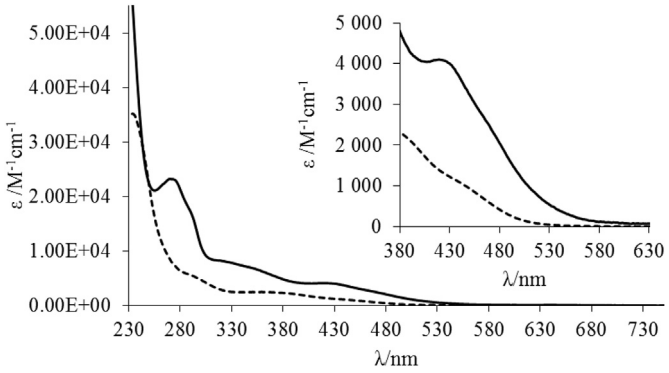

Fig. 1. UV–visible spectrum in CH_2Cl_2 for complexes **Ru1** (- - - -) and **Ru2** (———).

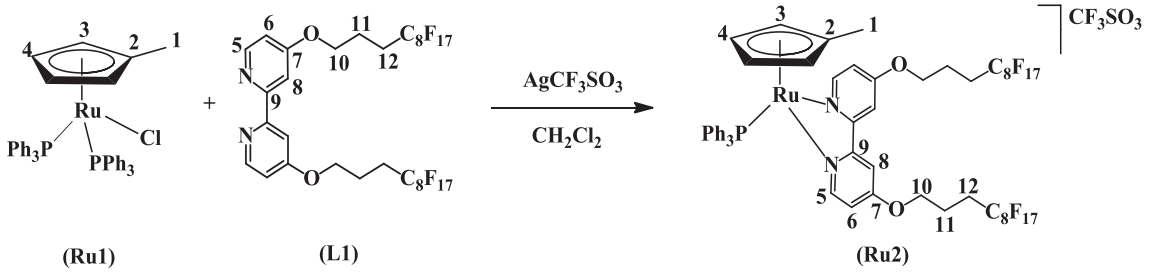

Scheme 1. Synthetic route of the new Ru(II) complex [Ru(η^5-MeCp)(PPh_3)(**L1**)][CF_3SO_3]; all compounds are numbered for NMR assignments.

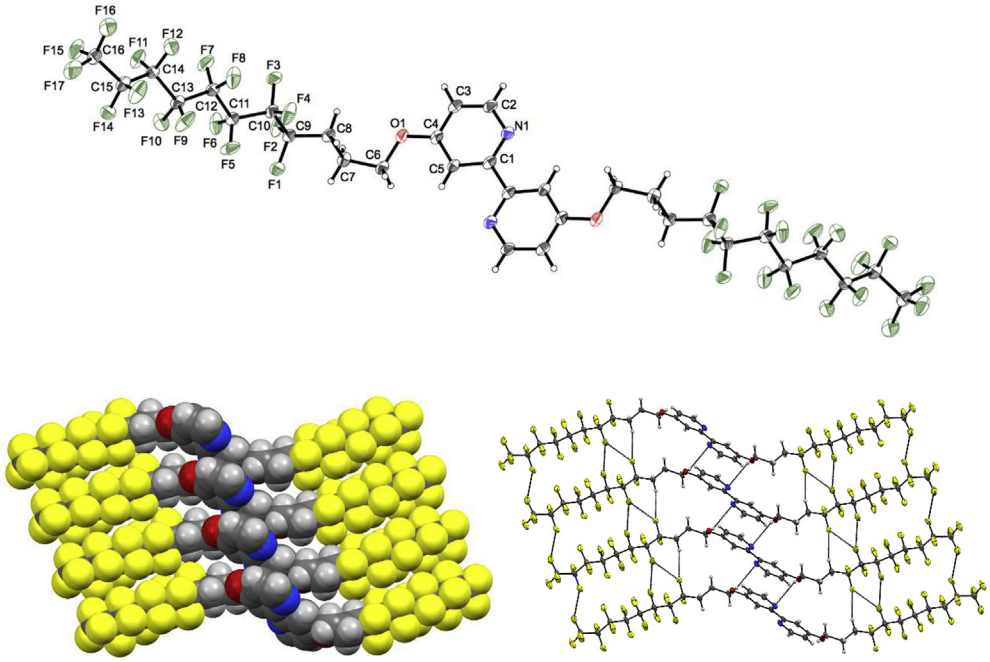

Fig. 2. Molecular structure (top) and packing (bottom) of **L1**. Thermal ellipsoids are drawn at 50% probability level.

In the case of **Ru2** another intense band at 290 nm from the π–π* electronic transitions occurring in the aromatic ring of **L1** is observed. In the visible range, **Ru2** presents an absorption band and a shoulder at 419 nm and ~470 nm, respectively, that can be attributed to charge transfer transitions between the *N,N*-bidentate ligand **L1** and the ruthenium centre (Fig. 1) as observed in related complexes [19,22,25]. No significant modifications on band positioning were noticed in both solvents.

3.2.2. Complexes stability in aqueous solutions and estimation of lipophilicity

Envisaging the use of these new compounds as cytotoxic agents and their study in human cancer cell lines, their stability and behaviour in aqueous solution was studied in DMSO and in culture cellular media, using 2% DMSO, by UV–Vis spectroscopy. DMSO is the co-solvent used in the biological assays in order to allow complete solubilization of the compounds. **Ru1** spectral changes were about 25 and 10% at 24 h in DMSO and DMSO/DMEM, respectively, probably due to hydrolysis of the Ru-Cl bond (Fig. S1). **Ru2** was found to be very stable with spectral changes lower than 6% over 24 h in both solutions (Fig. S2).

The importance of hydrophobicity/lipophilicity of the compounds for medicinal purposes is a key feature in the development of new drugs since it affects their tissue permeability, binding to biomolecules, between others. In this frame, the *n*-octanol/water partition coefficient was measured using the shake-flask method,

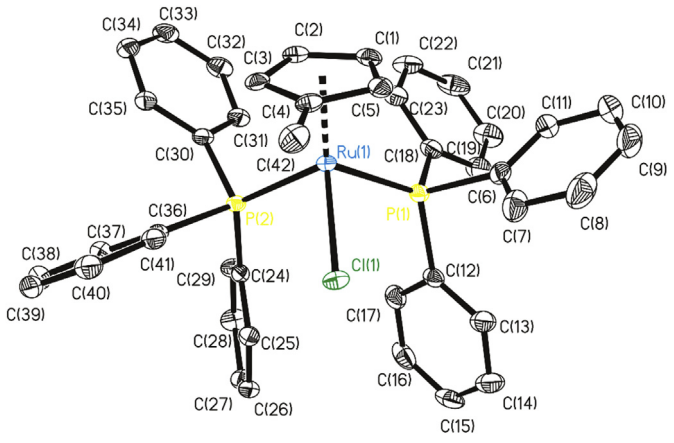

Fig. 3. ORTEP plot for the complex [Ru(MeCp)(PPh$_3$)$_2$Cl] (**Ru1**). All the non-hydrogen atoms are presented by their 50% probability ellipsoids. Hydrogen atoms are omitted for clarity.

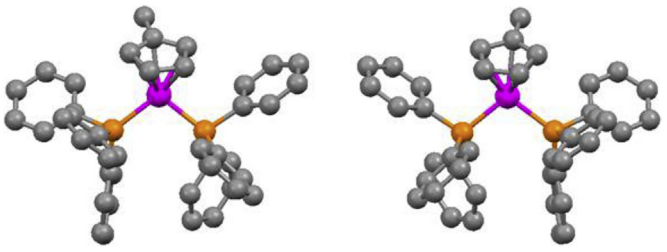

Fig. 4. Two enantiomers of the complex [Ru(MeCp)(PPh$_3$)$_2$Cl] (**Ru1**) present in the racemic crystal packing. View through the Ru-Cl edge. Drawing was done with Mercury 2.3 program in balls and sticks.

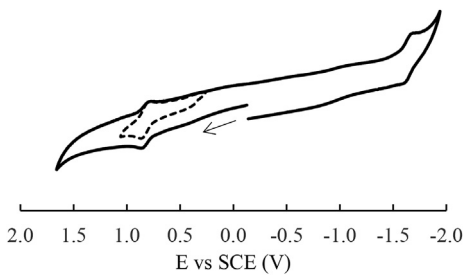

Fig. 5. Cyclic voltammogram of complex **Ru2** in acetonitrile, at 100 mV/s, showing the reversibility of the isolated oxidative process (dashed line).

Table 3
Electrochemical data for complexes **Ru1** and **Ru2** (all values *vs.* SCE, v = 100 mV.s^{-1}).

	E_{pa} (V)	E_{pc} (V)	$E_{1/2}$ (V)	$E_{pa} - E_{pc}$ (mV)	I_{pc}/I_{pa}
	Dichloromethane				
[Ru(η^5-MeCp)(PPh_3)$_2$Cl] (**Ru1**)	1.67	___	___	___	___
	1.41	___	___	___	___
	0.51	0.43	0.47	80	1.0
[Ru(η^5-MeCp)(PPh_3)(**L1**)][CF_3SO_3] (**Ru2**)	0.90	0.81	0.85	90	1.0
[RuCp(PPh_3)(2,2′-bipy)][CF_3SO_3] [25]	1.70	___	___	___	___
	1.53	___	___	___	___
	1.10	1.01	1.05	90	0.9
	Acetonitrile				
[Ru(η^5-MeCp)(PPh_3)$_2$Cl] (**Ru1**)	0.54	0.46	0.50	80	1.0
[Ru(η^5-MeCp)(PPh_3)(**L1**)][CF_3SO_3] (**Ru2**)	0.87	0.79	0.83	80	1.0
	−1.59	___	___	___	___
[RuCp(PPh_3)(2,2′-bipy)][CF_3SO_3] [25]	0.92	0.84	0.88	80	0.75

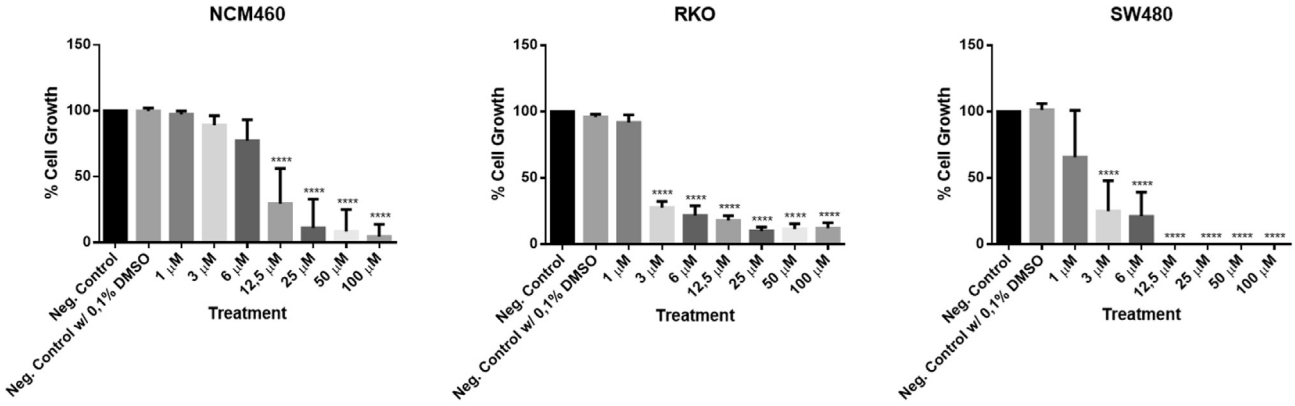

Fig. 6. Effects of **Ru2** compounds on cell growth of NCM460 normal colon epithelial mucosa derived cell line and RKO and SW480 colorectal cancer derived cell lines, determined by SRB assay. The percentage of cell growth relatively to the negative control was determined after a period of 48 h of exposure to the compounds and is expressed as a mean ± SD for each treatment from at least three independent experiments. Statistical analyzes was performed by one-way ANOVA comparing all conditions with negative control. The results were statistically significant with values of $p < 0.0001$ (****) ($n = 3$).

at room temperature. It was not possible to get an exact value for **Ru1** due to the spectral changes caused by the hydrolysis of the Ru-Cl bond, however, analysis of the spectra in octanol showed that it has a lipophilic character, since all the compound remained in this fraction. **Ru2** is also lipophilic ($logP_{o/w} = 0.25$; calibration curve in Fig. S3), as predictable by the known lipid solubility introduced by fluorine atoms.

3.3. Single crystal structure of *L1* and [Ru(η^5-MeCp)(PPh_3)$_2$Cl]·CH_2Cl_2 *Ru1*

Single crystals of **L1** were obtained by slow evaporation of chloroform at room temperature. Upon X-ray diffraction, it was revealed that the crystal of **L1** belongs to the centrosymmetric triclinic space group $P\bar{1}$. The asymmetric unit contains only half of the ligand molecule. The crystal packing shows intermolecular F···F (2.799–2.871 Å) interactions along with weak aliphatic C–H···N (2.662 Å) hydrogen bonds (Fig. 2). Table S1 contains selected bond lengths and angles for compound **L1**.

[Ru(MeCp)(PPh_3)$_2$Cl]·CH_2Cl_2 **Ru1** crystallizes from dichloromethane solution as red blocks (crystal dimensions 0.30 × 0.21 × 0.18 mm). Fig. 3 shows an ORTEP representation of [Ru(MeCp)(PPh_3)$_2$Cl] **Ru1.** The asymmetric unit contains for **Ru1** one ruthenium complex and one CH_2Cl_2 molecule. In the molecular structure, the ruthenium centre adopts a "piano stool" distribution formed by the ruthenium-MeCp unit bound to two phosphane ligands. One chloride ion occupies the other coordination position. X-ray structure analysis of **Ru1** shows two enantiomers of the complex [Ru(MeCp)(PPh_3)$_2$Cl] (**Ru1**) in the racemic crystal (space group $P\bar{1}$), the chirality being due to a twist of the PPh_3 and Cp units. The complex [Ru(MeCp)(PPh_3)$_2$Cl] (**Ru1**) presents a mirror plane which contain Cl, Ru and the centroid of Cp ring (see Fig. 4) [22,48]. The distances for Ru-P bond are Ru(1)-P(1) = 2.3132(6) Å and Ru(1)-P(2) = 2.3204(6) Å. The distance between Ru and the centroid of the π-bonded cyclopentadienyl moiety is 1.842(30) Å to Ru centre (ring slippage 0.079 Å). The mean value of the Ru-C bond distance is 2.2048(2) Å. Table S2 contains selected bond lengths and angles for compound **Ru1**.

Table 4
IC_{50} values determined by SRB assay after 48 h of incubation with **Ru2** and cisplatin in NCM460, RKO and SW480 cell lines. Values represent mean ± SD of at least three independent experiments.

	Ru2 (μM)	Cisplatin (μM)
NCM460	8.7 ± 0.9	–
RKO	2.0 ± 0.2	12.5 ± 1.2
SW480	1.5 ± 0.3	7.0 ± 0.1

3.4. Electrochemical studies

The redox behaviour of complex [Ru(η^5-MeCp)(PPh_3)(**L1**)][CF_3SO_3] **(Ru2)** and the precursor [Ru(η^5-MeCp)(PPh_3)$_2$Cl] (**Ru1**) was studied by cyclic voltammetry in dichloromethane and acetonitrile solutions, containing ammonium hexafluorophosphate as supporting electrolyte, between the limits imposed by the solvents (Table 2).

Complex **Ru1** showed to be redox-active in both solvents, with ruthenium centered processes (oxidation) at 0.54 V (ACN) and 0.51 V (DCM) with i_{pc}/i_{pa} ratios of 0.7, suggesting some instability of the oxidized ruthenium species at the electrode surface. However, when the scan direction is immediately reverted after the oxidation potential, the processes became quasi-reversible ($E_{1/2} = 0.50$ V and $E_{1/2} = 0.47$ V for acetonitrile and dichloromethane, respectively). In dichloromethane, this ruthenium centered process is followed by two other irreversible oxidative processes, also found in similar compounds [25], and probably originated by the oxidation of species resulting of the first Ru^{II}/Ru^{III} oxidation process.

In a 0.1 M [n-Bu_4N][PF_6]/acetonitrile solution (Fig. 5), complex **Ru2** was characterized by a quasi-reversible ruthenium centered process at $E_{1/2} = 0.83$ V and an irreversible reduction at $E_{pc} = -1.69$ V, which can be attributed to a ligand-based process. The electrochemical response of **Ru2** in dichloromethane is consistent with the behaviour observed in acetonitrile, with a quasi-reversible redox process at $E_{1/2} = 0.855$ V, found when the

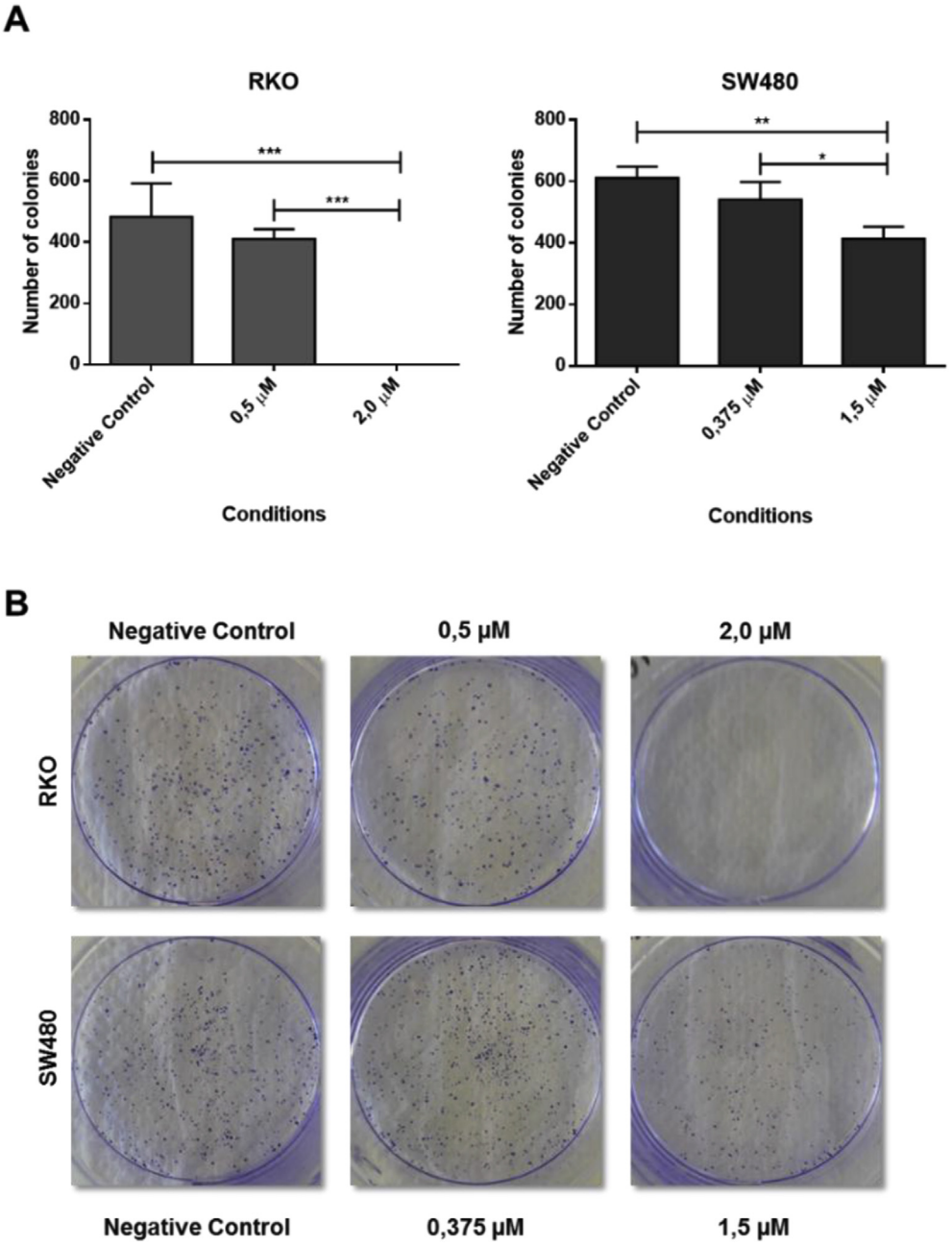

Fig. 7. Colony formation assay of RKO and SW480 cell lines after exposure with Ru2. (**A**) Analysis of the clonogenic ability, after 48 h of incubation with ¼ IC_{50} and IC_{50}, in RKO and SW480 cell lines. Values represent mean ± S.D. of at least three independent experiments. Statistical analysis was performed by one-way ANOVA with Turkey's multiple comparisons test. *P = 0.05; **P = 0.01; ***P = 0.001 compared with negative control. (**B**) Representative images of colony formation assay in RKO and SW480 cell lines.

scan direction is reverted after the oxidation potential and attributed to the Ru(II)/Ru(III) redox couple.

The oxidation potential found for the Ru(II)/Ru(III) redox pair is lower than the one found for the related [Ru(η^5-C_5H_5)(PPh_3)(2,2′-bpy)][CF_3SO_3] complex ($E_{1/2}$ = 1.05 V) [25] in the same experimental conditions (Table 3), indicating that the substitution of the cyclopentadienyl ring by the electron donor methyl group influences the electronic capability of the ruthenium(II) centre, making easier the oxidation process.

3.5. *In vitro cytotoxicity analysis and IC_{50} determination*

Colorectal cancer (CRC) derived cell lines RKO and SW480, as well as NCM460, a noncancerous cell line derived from normal colon epithelial cells, were incubated for 48 h with different concentrations of **Ru1** and **Ru2** compounds to assess cell growth by Sulphorhodamine B (SRB) assay. Compound **L1** could not be tested since its solubility in cellular media (and DMSO) is very limited. **Ru1** compound had no significant effect at the concentrations tested compared to the negative controls in the three cell lines (Fig. S3). **Ru2** proved to be a very active compound in colorectal cancer cell lines showing a significant decrease in cell growth even for low doses and not exhibiting a significant effect on the noncancerous cell line NCM460 that showed to be more resistant (Fig. 6). **Ru2** compound affects the growth of these cells in values in the micromolar range. The half-maximal inhibitory concentration

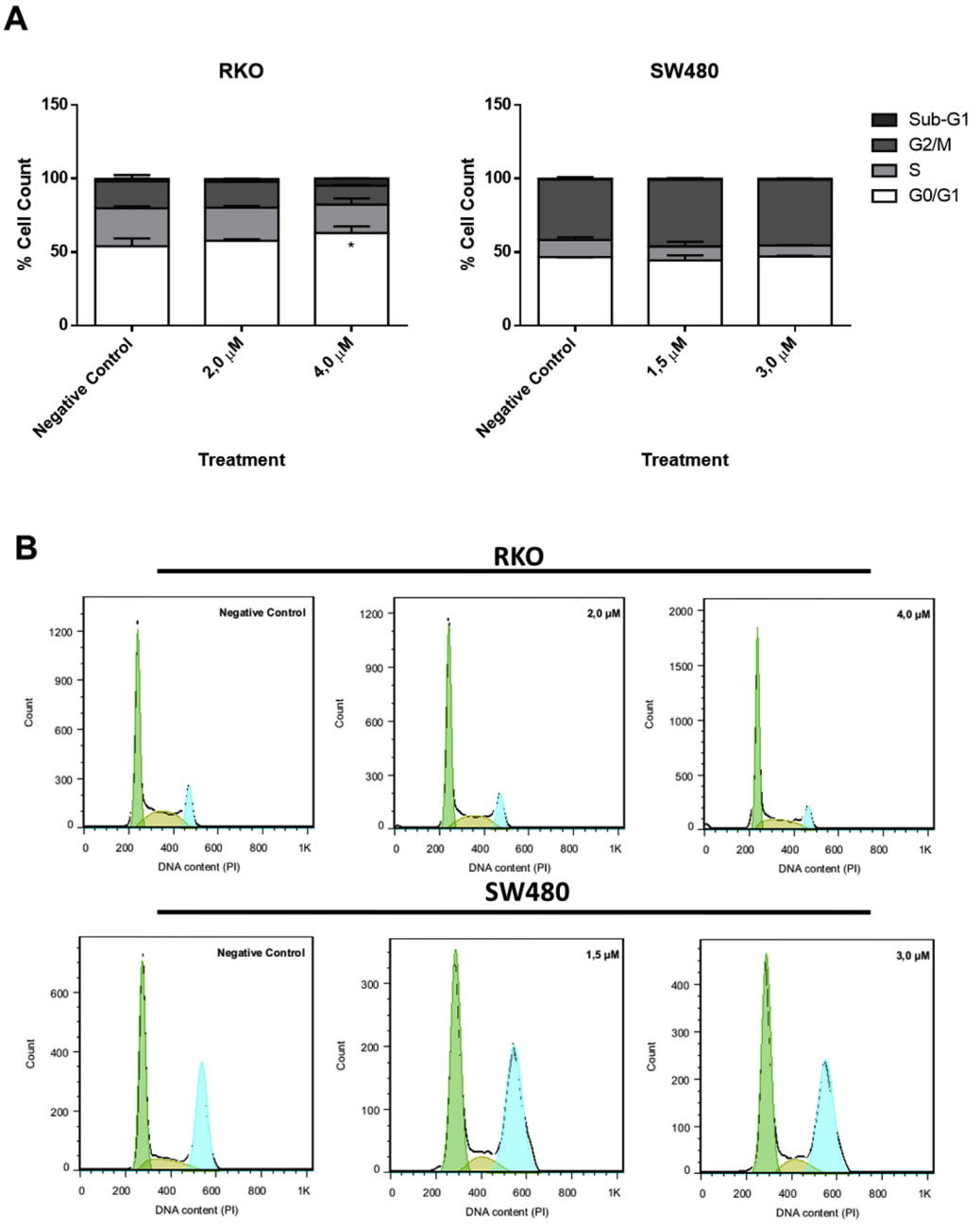

Fig. 8. Ru2 interfere with cell cycle in RKO colorectal cancer cell lines. (**A**) Analysis of the distribution of cell-cycle phases by flow cytometry, after 48 h of incubation with IC_{50} and 2 × IC_{50}, in RKO and SW480 cell lines. Values represent mean ± S.D. of at least three independent experiments. Statistical analysis was performed by multiple t-tests. *P = 0.05 compared with negative control. (**B**) Representative histograms of PI staining in RKO and SW480 were performed using FlowJo 7.6 software.

(IC_{50}) of **Ru2** was therefore calculated from statistical analyses of the mean values of SRB for all lines analyzed using GraphPad Prism 6 software. The IC_{50} values for RKO and SW480, were 2 μM and 1.5 μM, respectively, being 4–6 times better than the positive control cisplatin, and for NCM460 cells the IC_{50} was 8.7 μM (Table 4, Fig. S4).

The results showed that for **Ru2** the colorectal cancer cellS, RKO and SW480, are more sensitive than NCM460 cells showing a lower IC_{50} than for the normal colon cells. The IC_{50} values obtained in the SW480 cell line are in the same range of those obtained for other ruthenium arene complexes with modified paullones [49] or 8-substituted indolo[3,2-*c*]quinolines [50] (IC_{50} = 0.64–4.1 or 0.13–5.0 μM at 96 h incubation, respectively) and are much better than indazolium *trans*-[tetrachlorobis(1H-indazole)ruthenate(III)] [51] (KP1019; 43 ± 8 at 96 h incubation).

3.6. Proliferation and apoptosis analysis

In order to evaluate the clonogenic ability of **Ru2** in RKO and SW480 a colony formation assay was performed using the ¼ IC_{50} and IC_{50} values. In both cell lines the **Ru2** compound affected the ability to form colonies in a dose-dependent manner (Fig. 7). **Ru2**, at a concentration of 2 μM (IC_{50}), inhibits the ability to produce colonies in the RKO cell line.

The cell cycle distribution was assessed by flow cytometry, after 48 h of exposure to the IC_{50} and 2 × IC_{50} values for RKO and SW480. Two peaks corresponding to the G0/G1 and G2/M phases of the cell cycle were evident in DNA content histograms (Fig. 8). Comparing with the negative control, the IC_{50} value does not affect the cell cycle phases, in the RKO cell line. However, the 2 × IC_{50} value led to an increase in the percentage of cells in G0/G1 cell cycle phase and, consequently, an arrest at that phase. Relatively to the hypodiploid sub-G1 cell-cycle phase, only for RKO, the 2 × IC_{50} value showed an increase in the percentage of cells (5%) comparing with the negative control (1.5%). SW480 did not show significant differences between treatments compared to the negative control.

We also assessed the levels of late apoptosis by TUNEL assay, after an incubation for 48 h with IC_{50} and 2 × IC_{50} values for both cell lines. In comparison to the negative control, there were significant increase in the number of TUNEL positive cells with 2 μM

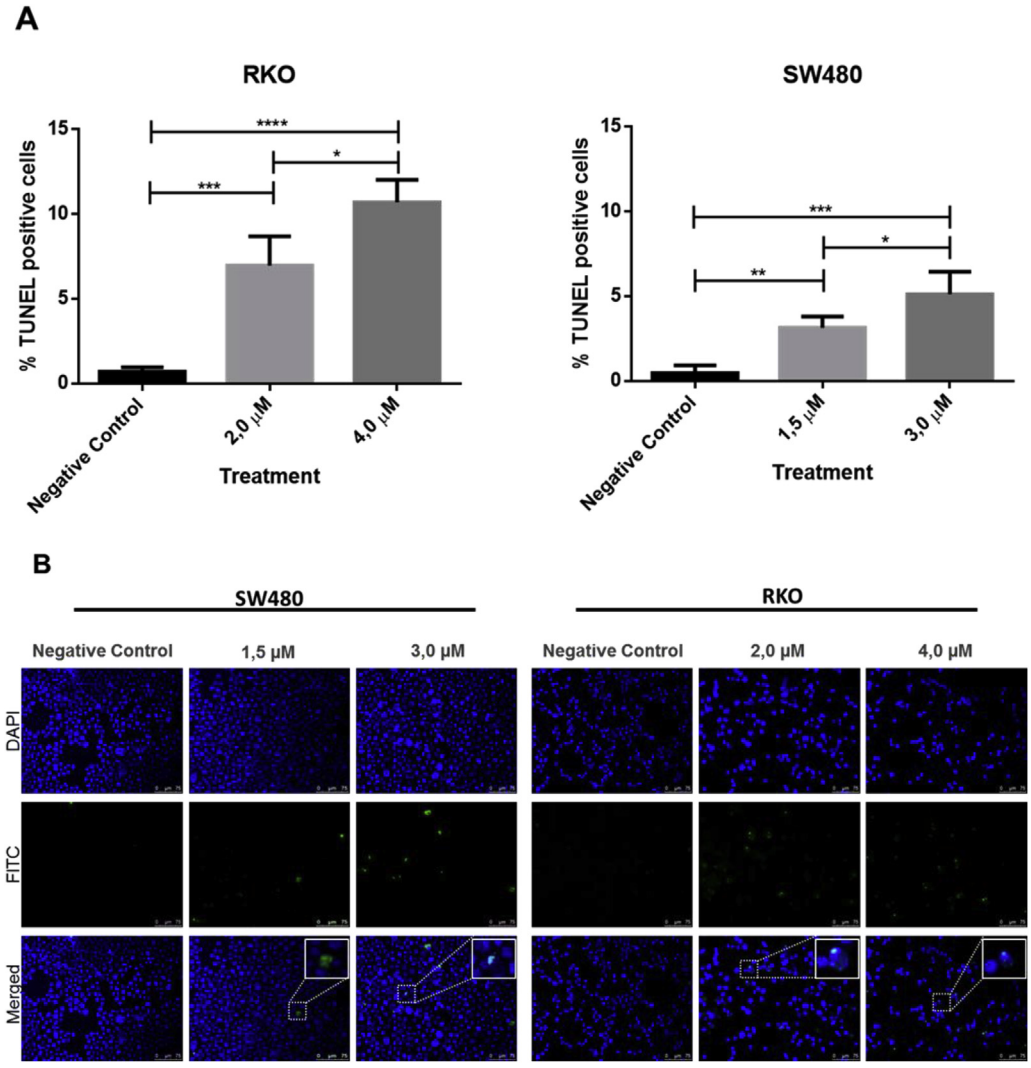

Fig. 9. Ru2 increases levels of TUNEL positive cells in colorectal cancer cell lines. RKO and SW480 cells were analyzed by TUNEL assay, after incubation with IC_{50} and 2 × IC_{50} concentrations for 48 h. (**A**) Analysis of TUNEL assay in RKO and SW480 cells. Values represent mean ± S.D. of at least three independent experiments. Statistical analysis was performed by one-way ANOVA with Turkey's multiple comparisons test. *P = 0.05; **P = 0.01; ***P = 0.001; ****P = 0.0001 compared with negative control. (**B**) Representative images (×200) of TUNEL assay. DAPI (4′,6-diamidino-2-phenylindole), FITC (fluorescein isothiocyanate) and merged were obtained by fluorescence microscopy.

and 4 μM (0.7% vs. 7% and 11%) for RKO and 1.5 μM and 3 μM (0.5% vs. 3% and 5%) for SW480 (Fig. 9). In both cell lines apoptotic bodies were observed, phenotypic alterations typical of apoptosis.

Our results suggest that **Ru2** seems to have more effect in RKO than in SW480 cells, which could be related with the different genetic background of the cells.

4. Conclusions

A new bipyridine-perfluorinared ligand **L1** and two ruthenium organometallic complexes, **Ru1** and **Ru2**, were newly synthesized and characterized. **L1** and **Ru1** were also studied by single-crystal X-ray. Both compounds crystalize in the centrosymmetric triclinic space group $P\bar{1}$. **Ru1** and **Ru2** cytotoxicity was evaluated in two human derived CRC cell lines, RKO and SW480, and in a noncancerous cell line, NCM460. While compound **Ru1** was not cytotoxic for any of the tested cell lines, compound **Ru2**, [Ru(η^5-MeCp)(PPh_3)(**L1**)][CF_3SO_3], inhibit cell growth of the two human colon cell lines tested at low IC_{50} doses (2 and 1.5 μM) in comparison with the normal colon derived cells NCM480 (IC_{50} = 8.7 μM). Moreover, **Ru2** could inhibit colony formation and induce apoptosis in CRC cell lines. Our results suggest that **Ru2** show an intrinsic selectivity towards cancer cells in relation to the normal colon epithelial derived cells which is approximately 4 times more resistant to the **Ru2** compound.

Overall, our results indicate that **Ru2** seems a very promising candidate for future studies aiming at understanding its mechanism of action in order to investigate its potential use as a new anticancer agent to be used at least in colorectal cancer therapy strategies.

Conflicts of interest

There are no conflicts of interest to declare.

Authors' contributions

R.G.T., A.S., L.CR., R.T., A.R.B., F.A. and T.M. performed experimental work and data analysis; M.P.R., A.P., M.H. and A.V. designed experiments; M.P.R., F.A., M.H.G., A.P., M.H. and A.V. wrote the paper. M.P.R., F.A., M.H.G, A.P., M.H. and A.V. did a critical revision.

Acknowledgements

This work was financed by the Portuguese Foundation for Science and Technology (Fundação para a Ciência e Tecnologia, FCT) within the scope of the strategic programmes UID/QUI/00100/2013 and UID/BIA/04050/2013 (POCI-01-0145-FEDER-007569) and by the ERDF through the COMPETE2020 - Programa Operacional Competitividade e Internacionalização (POCI). Andreia Valente and Anabela Sanches acknowledge the Investigator FCT2013 Initiative for the project IF/01302/2013 (acknowledging FCT, as well as POPH and FSE - European Social Fund). AV acknowledges the Royal Society of Chemistry's Research Fund. Leonor Côrte-Real thanks FCT for her Ph.D. Grant (SFRH/BD/100515/2014). The authors acknowledge the COST action CM1302 (SIPs).

Abbreviations

ATCC	American Type Culture Collection
DMEM	Dulbecco's Modified Eagle Medium
DMSO	Dimethyl sulfoxide
FBS	Fetal Bovine Serum
IC_{50}	Half-maximal inhibitory concentration
MeCp	methylcyclopentadienyl
RPMI	Roswell Park Memorial Institute Medium
SRB	Sulphorhodamine B

Appendix A. Supplementary data

Supplementary data related to this article can be found at https://doi.org/10.1016/j.ejmech.2017.11.059.

References

[1] S. Komeda, A. Casini, Curr. Top. Med. Chem. 12 (2012) 219–235.
[2] W.M. Motswainyana, P.A. Ajibade, Adv. Chem. 2015 (2015) 1–21.
[3] G. Palermo, A. Magistrato, T. Riedel, T. von Erlach, C.A. Davey, P.J. Dyson, U. Rothlisberger, ChemMedChem (2016) 1199–1210.
[4] W. Zheng, Y. Zhao, Q. Luo, Y. Zhang, K. Wu, F. Wang, Sci. China Chem. 59 (2016) 1240–1249.
[5] B.S. Murray, M.V. Babak, C.G. Hartinger, P.J. Dyson, Coord. Chem. Rev. 306 (2016) 86–114.
[6] T.S. Morais, A. Valente, A.I. Tomaz, F. Marques, M.H. Garcia, Future Med. Chem. 8 (2016) 527–544.
[7] C. Scolaro, A. Bergamo, L. Brescacin, R. Delfino, M. Cocchietto, G. Laurenczy, T.J. Geldbach, G. Sava, P.J. Dyson, J. Med. Chem. 48 (2005) 4161–4171.
[8] R.E. Morris, R.E. Aird, S. Murdoch, H. Chen, J. Cummings, N.D. Hughes, S. Parsons, A. Parkin, G. Boyd, D.I. Jodrell, P.J. Sadler, J. Med. Chem. 6 (2001) 3616–3621.
[9] A. Bergamo, A. Masi, A.F.A. Peacock, A. Habtemariam, P.J. Sadler, G. Sava, J. Inorg. Biochem. 104 (2010) 79–86.
[10] H. Bregman, E. Meggers, Org. Lett. 8 (2006) 5465–5468.
[11] J. Maksimoska, L. Feng, K. Harms, C. Yi, J. Kissil, R. Marmorstein, E. Meggers, J. Am. Chem. Soc. 130 (2008) 15764–15765.
[12] E.K. Martin, N. Pagano, M.E. Sherlock, K. Harms, E. Meggers, Inorg. Chim. Acta 423 (2014) 530–539.
[13] M. Serrano-Ruiz, L.M. Aguilera-Sáez, P. Lorenzo-Luis, J.M. Padrón, A. Romerosa, Dalton Trans. 42 (2013) 11212–11219.
[14] A. Romerosa, M. Saoud, T. Campos-Malpartida, C. Lidrissi, M. Serrano-Ruiz, M. Peruzzini, J.A. Garrido, F. García-Maroto, Eur. J. Inorg. Chem. (2007) 2803–2812.
[15] A. Romerosa, T. Campos-malpartida, C. Lidrissi, M. Saoud, M. Serrano-ruiz, M. Peruzzini, J.A. Garrido-ca, F. Garcı, Ä. De Quı, C. Organometallici, V. Madonna, F. Fi, Ä. De Bioquı, F. De Ciencias, U.V. De Almerı, Inorg. Chem. 45 (2006) 1289–1298.
[16] C. Ríos-luci, L.G. León, A. Mena-cruz, E. Pérez-roth, P. Lorenzo-luis, A. Romerosa, J.M. Padrón, Bioorg. Med. Chem. Lett. 21 (2011) 4568–4571.
[17] Z. Mendoza, P. Lorenzo-Luis, M. Serrano-Ruiz, E. Martín-Batista, J.M. Padrón, F. Scalambra, A. Romerosa, Inorg. Chem. 2 (2016) 7820–7822.
[18] L. Hajji, C. Saraiba-Bello, A. Romerosa, G. Segovia-Torrente, M. Serrano-Ruiz, P. Bergamini, A. Canella, Inorg. Chem. 50 (2011) 873–882.
[19] T.S. Morais, F.C. Santos, T.F. Jorge, L. Côrte-Real, P.J.A. Madeira, F. Marques, M.P. Robalo, A. Matos, I. Santos, M.H. Garcia, J. Inorg. Biochem. 130 (2014) 1–14.
[20] P.R. Florindo, D.M. Pereira, P.M. Borralho, C.M.P. Rodrigues, M.F.M. Piedade, A.C. Fernandes, J. Med. Chem. 58 (2015) 4339–4347.
[21] T.S. Morais, T.J.L. Silva, F. Marques, M.P. Robalo, F. Avecilla, P.J.A. Madeira, P.J.G. Mendes, I. Santos, M.H. Garcia, J. Inorg. Biochem. 114 (2012) 65–74.
[22] L. Côrte-Real, M. Paula Robalo, F. Marques, G. Nogueira, F. Avecilla, T.J.L. Silva, F.C. Santos, A. Isabel Tomaz, M. Helena Garcia, A. Valente, J. Inorg. Biochem. 150 (2015) 148–159.
[23] A. Valente, M.H. Garcia, F. Marques, Y. Miao, C. Rousseau, P. Zinck, J. Inorg. Biochem. 127 (2013) 79–81.
[24] M. Helena Garcia, T.S. Morais, P. Florindo, M.F.M. Piedade, V. Moreno, C. Ciudad, V. Noe, J. Inorg. Biochem. 103 (2009) 354–361.
[25] V. Moreno, M. Font-Bardia, T. Calvet, J. Lorenzo, F.X. Avilés, M.H. Garcia, T.S. Morais, A. Valente, M.P. Robalo, J. Inorg. Biochem. 105 (2011) 241–249.
[26] T.S. Morais, F. Santos, L. Côrte-Real, F. Marques, M.P. Robalo, P.J.A. Madeira, M.H. Garcia, J. Inorg. Biochem. 122 (2013) 8–17.
[27] M. Fernández, E. Rodríguez, C. Sarniguet, T.S. Morais, A. Isabel, C. Olea, R. Figueroa, J.D. Maya, A. Medeiros, M. Comini, M.H. Garcia, L. Otero, D. Gambino, J. Inorg. Biochem. 153 (2015) 306–314.
[28] P.R. Florindo, D.M. Pereira, M.P. Borralho, P.J. Costa, M.F.M. Piedade, C.M.P. Rodrigues, A.C. Fernandes, Dalt. Trans. 45 (2016) 11926–11930.
[29] V. Moreno>, J. Lorenzo, F.X. Aviles, M.H. Garcia, J.P. Ribeiro, T.S. Morais, P. Florindo, M.P. Robalo, Bioinorg. Chem. Appl. (2010), 936834, 11 pages.
[30] N. Mendes, F. Tortosa, A. Valente, F. Marques, A. Matos, T.S. Morais, A.I. Tomaz, F. Gärtner, M.H. Garcia, Anticancer. Agents Med. Chem. 17 (2017) 126–136.
[31] W.K. Hagmann, J. Med. Chem. 51 (2008) 4359–4369.
[32] P. Shah, A.D. Westwell, J. Enzyme Inhib. Med. Chem. 22 (2007) 527–540.
[33] D.B. Longley, D.P. Harkin, P.G. Johnston, Nat. Rev. Cancer 3 (2003) 330–338.
[34] C.M. Clavel, E. Păunescu, P. Nowak-Sliwinska, P.J. Dyson, Chem. Sci. 5 (2014) 1097.
[35] P. Nowak-Sliwinska, C.M. Clavel, E. Paŧunescu, M.T. Te Winkel, A.W. Griffioen, P.J. Dyson, Mol. Pharm. 12 (2015) 3089–3096.
[36] A.K. Renfrew, R. Scopelliti, P.J. Dyson, Inorg. Chem. 49 (2010) 2239–2246.

[37] R. Prasad, R. Shikha, S. Mukhopadhyay, G. Sharma, B. Koch, P. Vishnoi, D. Shankar, Inorg. Chim. Acta 454 (2017) 117–127.
[38] W.L.F. Armarego, C.L.L. Chai, Purif. Lab. Chem. (2009) 61–79.
[39] R. Tatikonda, S. Bhowmik, K. Rissanen, M. Haukka, M. Cametti, Dalt. Trans. 45 (2016) 12756–12762.
[40] M.I. Bruce, N.J. Windsor, Aust. J. Chem. 30 (1977) 1601–1604.
[41] Rigaku Oxford Diffraction, CrysAlisPro, Agilent Technologies inc., Yarnton, Oxfordshire, England, 2013.
[42] L. Palatinus, G. Chapuis, J. Appl. Crystallogr. 40 (2007) 786–790.
[43] G.M. Sheldrick, Acta Crystallogr. Sect. C Struct. Chem. 71 (2015) 3–8.
[44] G.M. Sheldrick, SADABS, version 2.10, University of Göttingen, Germany, 2004.
[45] G.M. Sheldrick, Acta Crystallogr. Sect. A A64 (2008) 112–122.
[46] A. Berthod, S. Carda-Broch, J. Chromatogr. A 1037 (2004) 3–14.
[47] M.P. Moyer, L. a Manzano, R.L. Merriman, J.S. Stauffer, L.R. Tanzer, In Vitro Cell. Dev. Biol. Anim. 32 (1996) 315–317.
[48] P. Govindaswamy, D. Linder, J. Lacour, G. Süss-Fink, B. Therrien, Dalton Trans. 6 (2007) 4457–4463.
[49] G. Mühlgassner, C. Bartel, W.F. Schmid, M.A. Jakupec, V.B. Arion, B.K. Keppler, J. Inorg. Biochem. 116 (2012) 180–187.
[50] L.K. Filak, S. Göschl, S. Hackl, M.A. Jakupec, V.B. Arion, Inorg. Chim. Acta 393 (2012) 252–260.
[51] C. Bartel, A.E. Egger, M.A. Jakupec, P. Heffeter, M. Galanski, W. Berger, B.K. Keppler, J. Biol. Inorg. Chem. 16 (2011) 1205–1215.